Electronic Supplementary Material (ESI) for Journal of Materials Chemistry A.
This journal is © The Royal Society of Chemistry 2020

Supporting Information

Phosphate Ions and Oxygen Defects Modulated Nickel Cobaltite Nanowires: A Bifunctional Cathode for Flexible Hybrid Supercapacitors and Microbial Fuel Cells

Wenda Qiu,‡*[ab] Quanhua Zhou,‡[a] Hongbing Xiao,[a] Chun Zhou,[a] Wenting He,[a] Yu Li,*[a] and Xihong Lu[b]

[a] *School of Eco-Environmental Technology, Guangdong Industry Polytechnic, 152 Xingang West Road, Guangzhou 510300, China.*

[b] *MOE of the Key Laboratory of Bioinorganic and Synthetic Chemistry, KLGHEI of Environment and Energy Chemistry, School of Chemistry, Sun Yat-Sen University, 135 Xingang West Road, Guangzhou 510275, China.*

**Corresponding Author. E-mail: qiuwd5@mail.sysu.edu.cn (W. Qiu); liyugq@hotmail.com (Yu Li)*

Calculations:

The specific or areal capacity can be calculated via the equation (1) and (2) as follows:

CV curves:

$$C_S = \frac{Q}{m} = \frac{S}{2vm} \qquad (1)$$

GCD curves:

$$C_S = \frac{Q}{m} = \frac{I\Delta t}{m} \qquad (2)$$

Where C_s (mAh g^{-1}) is the specific capacity; Q (C) is the average charge during the charging and discharging process; m (g) is the mass loading of the active materials; S

(A V) is the integrated area of the CV curve; v (V/s) is the scan rate; I (A) is the constant discharging current; Δt (s) is the discharging time.

Energy density and power density were calculated by using the following equation (3) and (4):

$$E = \int_0^{\Delta t} IV(t)dt/m \qquad (3)$$

$$P = \frac{E}{1000 \times \Delta t} \qquad (4)$$

Where E (Wh kg^{-1}) is the energy density, P is the power density (kW kg^{-1}), V (V) is the potential window, I (mA) is the discharging current, m (g) is the total mass of active materials of the device, and $\triangle t$ (h) is the discharging time.

Balance the charge of electrodes in HSCs device:

As for a SC, the charge balance will follow the relationship $q^+= q^-$. The charge stored by each electrode depends on the capacity (C_s), the potential range for the charge/discharge process (ΔE) and the area of the electrode (A) following the Equation 10:

$$q = C_S \times \Delta E \times A \qquad (10)$$

To obtain $q^+= q^-$ at 100 mV s^{-1}, the area balancing between PNCO$_x$ and 3DPG will be calculated as follow:

$$\frac{A_{PNCOx}}{A_{3DPG}} = \frac{C_{(3DPG)} \times \Delta E_{3DPG}}{C_{PNCOx} \times \Delta E_{PNCOx}} \approx \frac{1}{1.12}$$

Therefore, the calculated areal ration between the PNCO$_x$ electrode and 3DPG electrode was about 1:1.12.

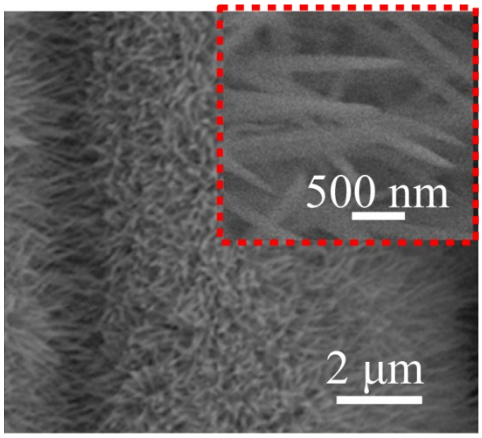

Figure S1. SEM images of the as-prepared NCO NWAs.

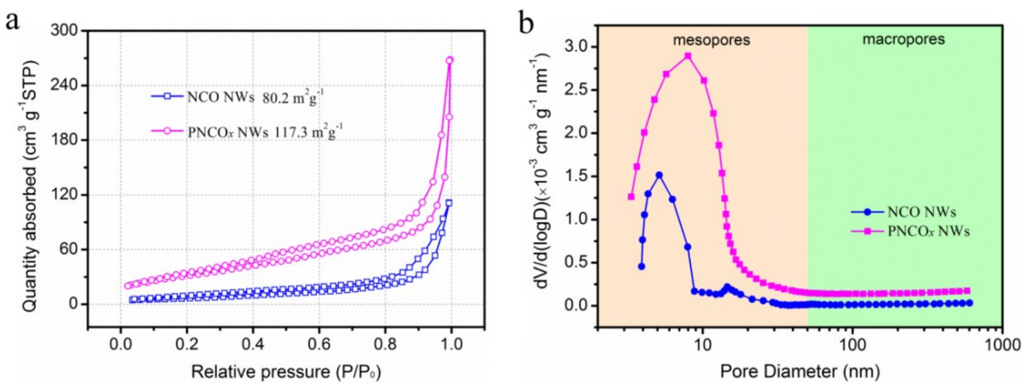

Figure S2. (a) N_2 adsorption/desorption isotherms and (b) pore-size distribution of the NCO NWs and PNCO$_x$ NWs.

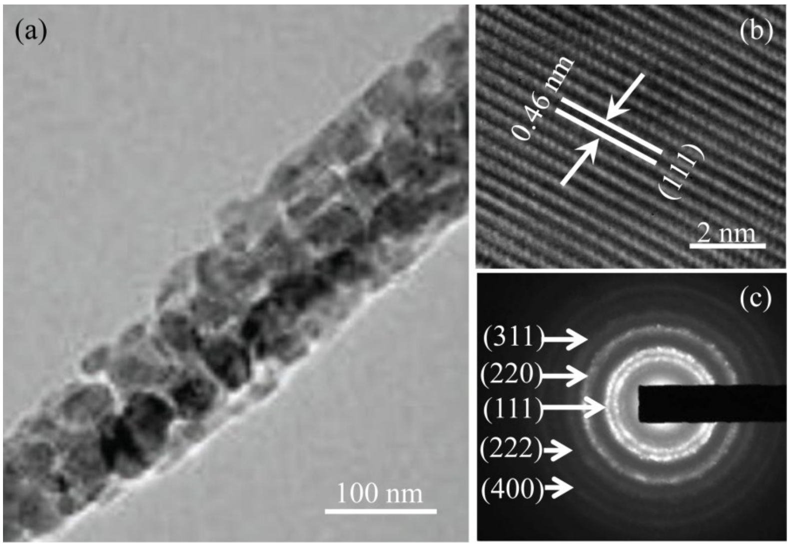

Figure S3. (a) TEM, (b) HRTEM, and (c) the corresponding SAED pattern of the pristine NCO NWs.

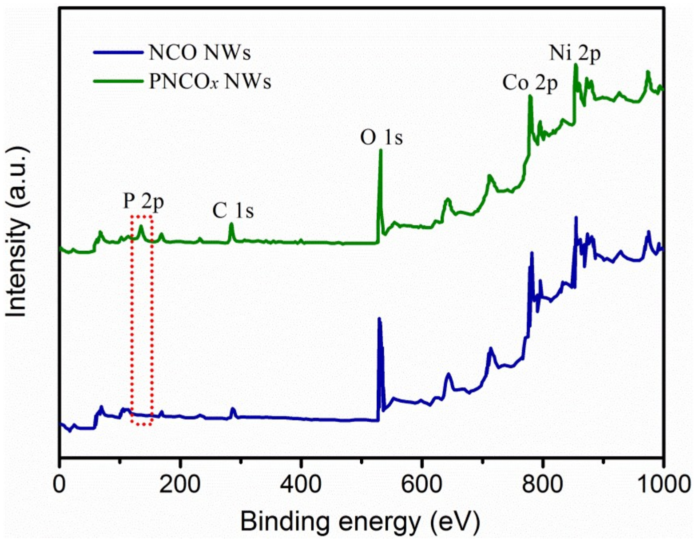

Figure S4. XPS survey spectra of NCO and PNCO$_x$ NWs.

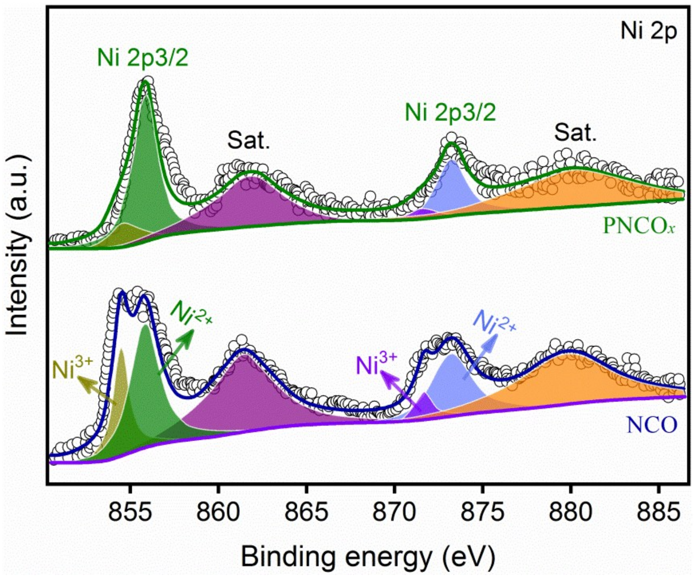

Figure S5. XPS survey of Ni 2p spectra for the pristine NCO and PNCO$_x$ NWs.

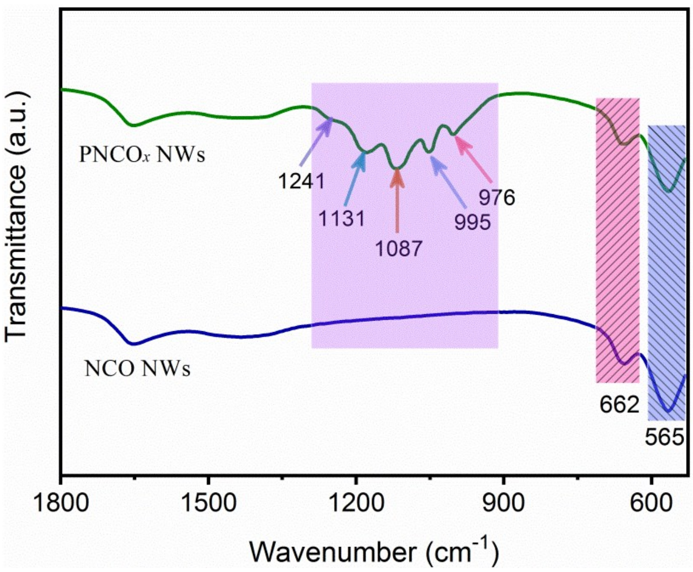

Figure S6. FTIR spectra of pristine NCO and PNCO$_x$ NWs.

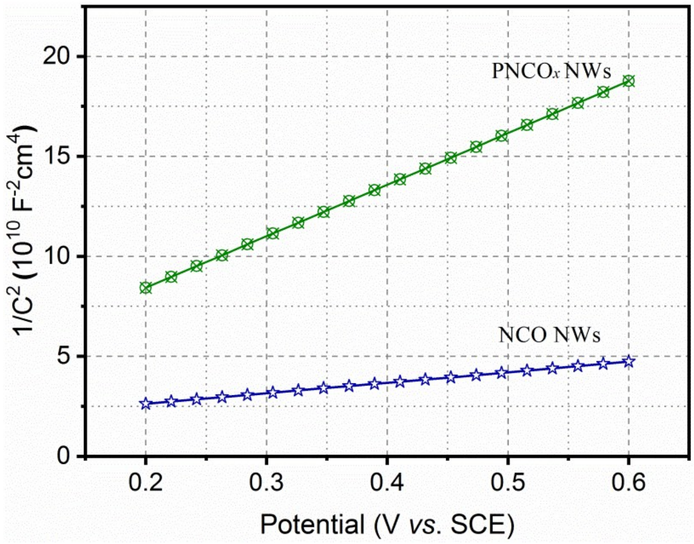

Figure S7. Mott-Schottky plots of pristine NCO and PNCO$_x$ NWs.

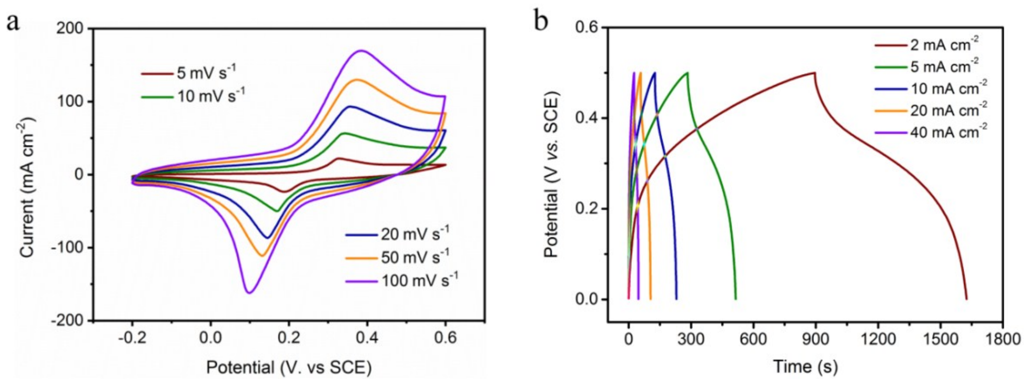

Figure S8. (a) CV curves of the PNCO$_x$ electrode collected at various scan rates. (b) GCD curves of the PNCO$_x$ electrode collected at different current density.

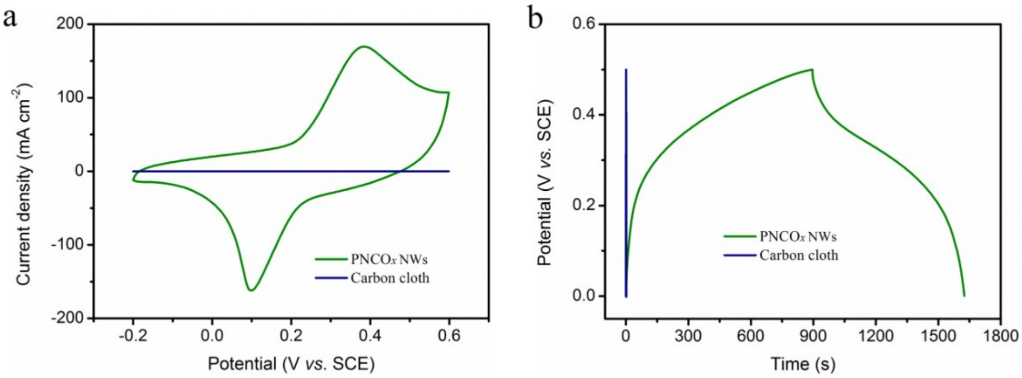

Figure S9. (a) CV and (b) GCD curves of the carbon cloth and PNCO$_x$ NWAs electrodes collected at 100 mV s^{-1} and 2 mA cm^{-1}, respectively.

Table S1. Electrochemical performance obtained from NCO based electrodes.

Type of electrode	capacity (mAh g^{-1})	Rate capability	Cyclability (cycles)	Ref.
PNCO$_x$ NWAs	686 (2 mA cm^{-1})	58% (2 to 40 mA cm^{-2})	96.5% (20000)	This work
NCO nanoneedle arrays	393 (1.11 mA cm^{-2})	18.91% (1.11 to 22.24 mA cm^{-2})	89.32% (2000)	1
Mesoporous NCO nanosheets	366 (1.8 mA cm^{-2})	39% (1.8 to 48.6 mA cm^{-2})	93% (3000)	2
NCO@$NiCo_2S_4$	260 (2 mA cm^{-1})	70.5% (2 to 20 mA cm^{-2})	65% (4000)	4
NCO/MCMF	257 (2 mA cm^{-2})	72.68% (2 to 40 mA cm^{-2})	85.8% (10000)	5
CC@NCO	176 (2.5 mA cm^{-1})	45.8% (2.5 to 60 mA cm^{-2})	No data	8

NCO nanosheets	168 (1.6 mA cm^{-2})	72.14% (1.6 to 16 mA cm^{-2})	No data	3
NCO-rGO	153 (1.25 mA cm^{-2})	62.84% (1.25 to 100 mA cm^{-2})	91.6% (3000)	7
NCO@$NiCo_2O_4$	143 (2 mA cm^{-2})	74.84% (2 to 40 mA cm^{-2})	96% (4000)	14
NCO–rGO	133 (2 mA cm^{-1})	69% (2 to 20 mA cm^{-2})	90% (5000)	11
NCO microspheres	131 (2.8 mA cm^{-2})	73% (2.8 to 56 mA cm^{-2})	93.6% (1600)	9
NCO/carbon textiles	120 (1.2 mA cm^{-1})	79% (1.2 to 24 mA cm^{-2})	No negligible (5000)	6
NCO–RGO	116 (2 mA cm^{-2})	73.65% (2 to 40 mA cm^{-2})	No negligible (4000)	13
Ni@NCO	113 (1.54 mA cm^{-2})	67.85% (1.54 to 30.8 mA cm^{-2})	93.2% (6000)	10
CC/NCO-S@NiO	105 (2 mA cm^{-1})	91.2% (2 to 16 mA cm^{-2})	100% (10000)	15
NCO nanospheres	94 (4 mA cm^{-2})	80% (4 to 40 mA cm^{-2})	No negligible (5000)	12
NCO	82 (1 mA cm^{-1})	80.55% (1 to 10 mA cm^{-2})	98.4% (1000)	16
NCO NWA	79 (0.5 mA cm^{-1})	47.09% (0.5 to 50 mA cm^{-2})	No data	17

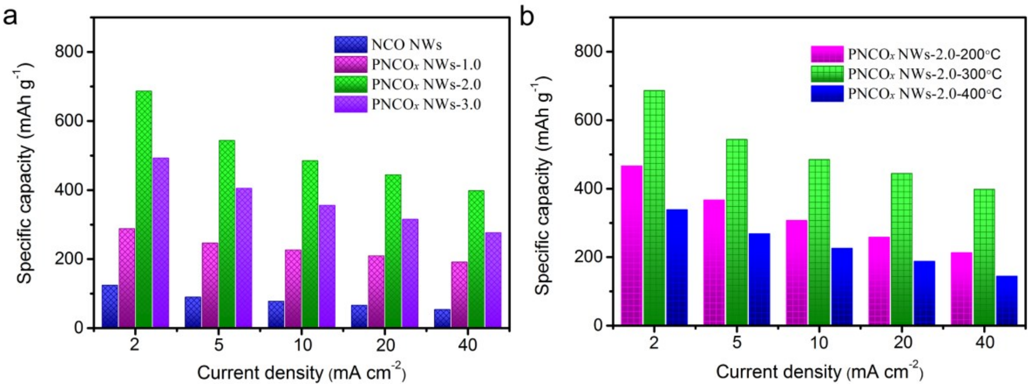

Figure S10. Specific capacity of PNCO$_x$ electrodes as a function of current densities with (a) different amount of $NaH_2PO_2 \cdot H_2O$ and (b) different annealing temperature.

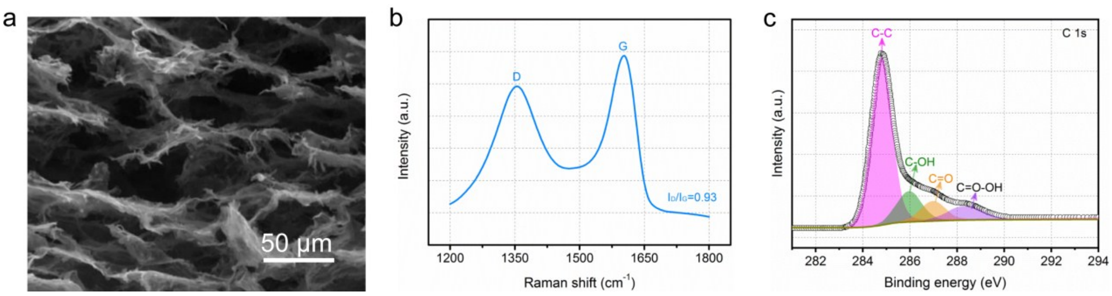

Figure S11. (a) SEM image, (b) Raman spectrum, and (c) C1s core-level XPS spectrum of 3DPG sample.

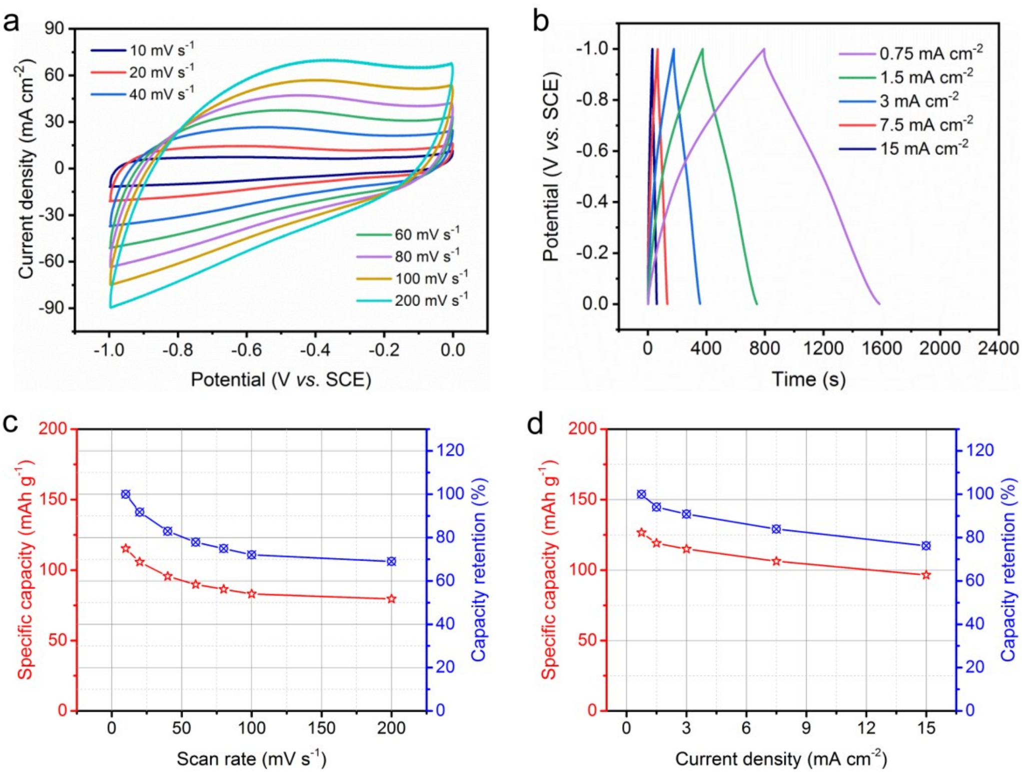

Figure S12. (a) CV curves for 3DPG electrode collected at different scan rates. (b) GCD curves of 3DPG electrode at various current densities. Sprcific capacity and capacity retention of 3DPG electrode as a function of (c) scan rate and (d) current density.

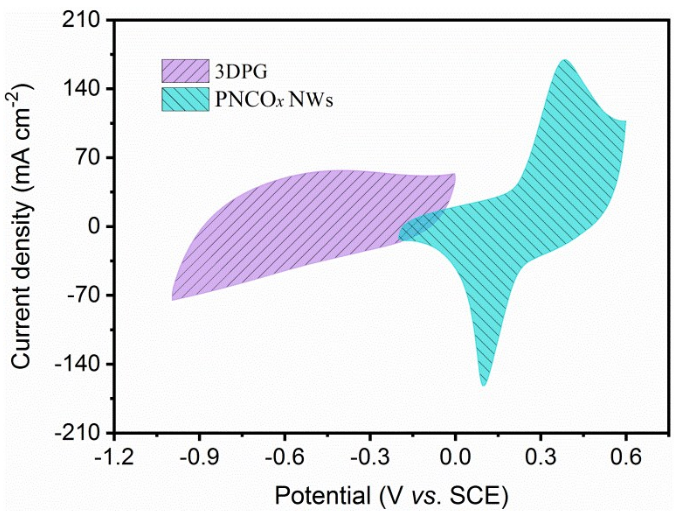

Figure S13. CV curves collected for 3DPG and PNCO$_x$ NWAs at the scan rate of 100 mV s^{-1}.

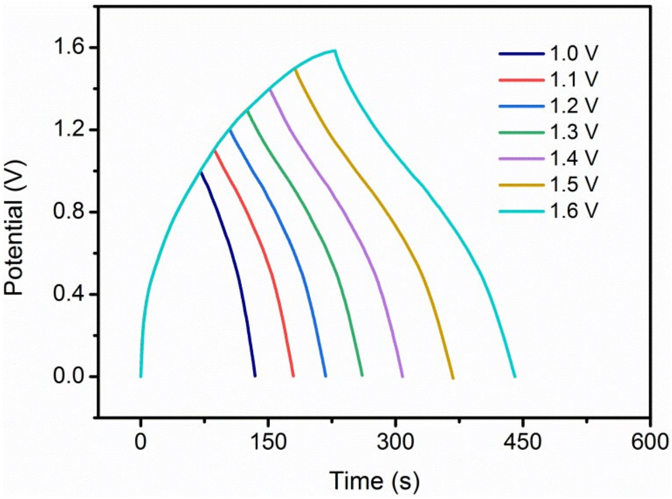

Figure S14. GCD curves of PNCO$_x$ NWAs//3DPG HSCs device collected at 5 mA cm^{-1} in the corresponding potential windows.

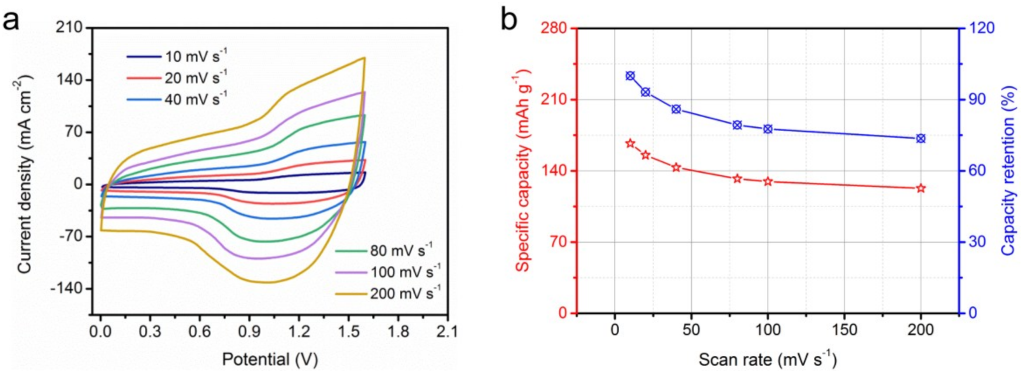

Figure S15. (a) CV curves for PNCO$_x$ NWAs//3DPG HSCs device collected at different scan rates. (b) Specific capacity and capacity retention of PNCO$_x$ NWAs//3DPG HSCs device as a function of scan rate.

Table S2. A comparison on the ORR activities of the recently reported catalysts.

catalysts	ORR E_{onset} (V *vs.* RHE)	ORR $E_{1/2}$ (V *vs.* RHE)	Electrolyte	Ref.
$PNCO_x$ NWAs	0.95	0.83	0.1 M KOH	This work
NC/Co-NGC DSNCs	0.92	0.82	0.1 M KOH	22
N, S-carbon nanosheet	0.92	0.77	0.1 M KOH	23
NCO/rGO	0.91	0.79	0.1 M KOH	18
CoO/N-graphene	0.90	0.81	0.1 M KOH	25
NCO NCs	0.86	0.674	0.1 M KOH	19
Co_3O_4/N-graphene	0.86	0.83	0.1 M KOH	26
Mn_xO_y/N-carbon	0.85	0.81	0.1 M KOH	24
$MnCo_2O_4$/NCNT	0.85	0.63	0.1 M KOH	27
Urchin like NCO	0.83	0.64	0.1 M KOH	21
Sphere like NCO	0.81	0.66	1 M NaOH	20
Ti_3C_2/g-C_3N_4	0.72	0.51	0.1 M KOH	28

References

1. G.Q. Zhang, H.B. Wu, H.E. Hoster, M.B. Chan-Park, X.W. Lou, *Energy Environ. Sci.*, 2012, **5**, 9453.
2. G.Q. Zhang, X.W. Lou, *Adv. Mater.,* 2013, **25**, 976.
3. H. Rong, T. Chen, R. Shi, Y.Y. Zhang, Z.H. Wang, *ACS Omega*, 2018, **3**, 5634.
4. Z.C. Qu, M.J. Shi, H.Z. Wu, Y.C. Liu, J.T. Jiang, C. Yan, *J. Power Sources*, 2019, **410**, 179.
5. C. Guan, X.M. Liu, W.N. Ren, X. Li, C.W. Cheng, J. Wang, *Adv. Energy Mater.*, 2017, **7**, 1602391.
6. C.Z. Yuan, J.Y. Li, L.R. Hou, X.G. Zhang, L.F. Shen, X.W. Lou, *Adv. Funct. Mater.,* 2012, **22**, 4592.
7. X. Wang, W.S. Liu, X.H. Lu, P.S. Lee, *J. Mater. Chem.* 2012, **22**, 23114.
8. X.Y. Liu, S.J. Shi, Q.Q. Xiong, L. Li, Y.J. Zhang, H. Tang, C.D. Gu, X.L. Wang, J.P. Tu, *ACS Appl. Mater. Interfaces*, 2013, **5**, 8790.
9. E. Umeshbabu, G. Rajeshkhanna, P. Justinb. G.R. Rao, *RSC Adv.*, 2015, **5**, 66657.
10. Y. Lei, Y.Y. Wang, W. Yang, H.Y. Yuan, D. Xiao, *RSC Adv.*, 2015, **5**, 7575.
11. L.F. Shen, Q. Che, H.S. Li, X.G. Zhang, *Adv. Funct. Mater.*, 2014, **24**, 2630.
12. H.W. Wang, Z.A. Hu, Y.Q. Chang, Y.L. Chen, H.Y. Wu, Z.Y. Zhang, Y.Y. Yang, *J. Mater. Chem.*, 2011, **21**, 10504.
13. G.X. Gao, H.B. Wu, S.J. Ding, L.M. Liu, X.W. Lou, *Small*, 2015, **11**, 804.
14. Y. Ouyang, R.J. Huang, X.F. Xia, H.T. Ye, X.Y. Jiao, L. Wang, W. Lei, Q.L. Hao, *Chem. Eng. J.*, 2019, **355**, 416.

15. M.J. Pang, S. Jiang, G.H. Long, Y. Ji, W. Han, B. Wang, X.L. Liu, Y.L. Xi, F.Z. Xu, G.D. Wei, *RSC Adv.*, 2016, **6**, 67839.

16. J.W. Xiao, S. H. Yang, *RSC Adv.*, 2011, **1**, 588.

17. Y.Y. Li, F. Tang, R.J. Wang, C. Wang, J.P. Liu, *ACS Appl. Mater. Interfaces*, 2016, **8**, 30232.

18. S. Liu, Z. Wang, S. Zhou, F. Yu, M. Yu, C. Y. Chiang, W. Zhou, J. Zhao, J. Qiu, *Adv. Mater.*, 2017, **29**, 1700874.

19. K. Qu, Y. Zheng, S. Dai, S.Z. Qiao, *Nano Energy*, 2016, **19**, 373.

20. T.W. Zhang, ZF Li, Z.X. Zhang, L.K. Wang, P. Sun, S.W Wang, *J. Phys. Chem. C*, 2018, **122**, 27469.

21. S. Mao, Z. Wen, T. Huang, Y. Hou, J. Chen, *Energy Environ. Sci.*, **2014**, 7, 609.

22. J. Li, S.Q. Lu, H.L. Huang, D.H. Liu, Z.B. Zhuang, C.L. Zhong, *ACS Sustainable Chem. Eng.*, 2018, **6**, 10021.

23. Y.Y. Liang, Y.G. Li, H.L. Wang, J.G. Zhou, J. Wang, T. Regier, H.J. Dai, *Nat. Mater.*, 2011, **10**, 780.

24. J. Masa, W. Xia, I. Sinev, A.Q. Zhao, Z.Y. Sun, S. Grützke, P. Weide, M. Muhler, W. Schuhmann, *Angew. Chem. Int. Ed.*, 2014, **53**, 8508.

25. A.Q. Zhao, J. Masa, W. Xia, A. Maljusch, M.G. Willinger, G. Clavel, K.P. Xie, R. Schlögl, W. Schuhmann, M. Muhler, *J. Am. Chem. Soc.*, 2014, **136**, 7551.

26. Z.Q. Liu, Q.Z. Xu, J.Y. Wang, N. Li, S.H. Guo, Y.Z. Su, H.J. Wang, J.H. Zhang, S. Chen, *Int. J. Hydrogen Energy*, 2013, **38**, 6657.

27. S.V. Devaguptapu, S. Hwang, S. Karakalos, S. Zhao, S. Gupta, D. Su, H. Xu, G.

Wu, *ACS Appl. Mater. Interfaces*, 2017, **9**, 44567.

28. T.Y. Ma, J.L. Cao, M. Jaroniec, S.Z. Qiao, *Angew. Chem. Int. Ed.*, 2015, **55**, 1138.